Full Paper

Feasibility of Detonation in Porous Silicon Nanoenergetics

Philip M. Guerieri,*[a] Brian Fuchs,[b] and Wayne A. Churaman[a]

Abstract: Porous silicon with sodium perchlorate oxidizer is hypothesized to be a detonable explosive, which is atypical for heterogenous fuel/oxidizer composites. The existence of detonation in energetic porous silicon remains contested and would theoretically feature several unique behaviors illustrated by this study. Calculations to predict detonation performance are performed using CHEETAH thermochemical code for silicon porosities of 45–85 % surrounding 69 %, which represents an experimentally typical case. Uniquely, e-PS detonation is predicted to produce low gas volume. At 69 % porosity, condensed detonation products comprise 78 % of the mass (varying from 86 % to 46 % for 45–85 % porosity), and therefore a low TNT equivalent mechanical energy of 0.429 (but 1.32 when comparing total detonation energy). The calculated pressure of detonation for 69 % porosity is 1.065 GPa, only about 4 % of that of typical military explosives but over 50 times greater than compression wave amplitudes estimated for fast-burning nanothermites, which are comparable heterogenous fuel/oxidizer composites. At porosities above 67 %, computed detonation velocities are shown to exceed estimates for the unreacted speed of sound and therefore a detonation structure consistent with classical CJ theory is proposed. Indeed, published maximum experimental propagation speeds for energetic porous silicon in this upper porosity range when pore size is optimal agree well with CHEETAH computations of detonation velocity, thereby supporting that detonation is possible. Below 66 % porosity, sound speed in unreacted material overtakes the calculated detonation velocities. Traditionally this precludes formation of a detonation wave since the shockwave would decay as energy propagates ahead acoustically into unreacted material. However, experimental agreement is still observed between 60–67 % porosity. By comparing computed detonation pressure with estimates for the strength of unreacted porous silicon, this range is proposed to be a transition zone in which a detonation-like structure could be maintained, despite the inverted sound speed comparison, by rapid catastrophic fracture of porous silicon at the detonation front. This hypothesis implies that a sonic precompression wave must precede the detonation wave since at least a minor fraction of shock energy would propagate ahead in unreacted material. Finally, comparisons are made with baseline primary explosives and nanothermites showing that among metal-based composite energetics on the basis of reaction rate and detonation pressure, energetic porous silicon currently exhibits the most promise for replacing primary explosives at reasonable densities in igniters and augmenting initiator formulations.

Keywords: Porous Silicon · Detonation · Energetic Materials · Initiation

1 Introduction

Nanoscale porosity can be etched top-down into a silicon substrate forming porous silicon (PS). When an oxidizer is introduced to the pore volume, the composite material is rendered reactive and termed ''energetic porous silicon" (e-PS), which is of interest due to the high quantity and rate of energy released [1]. e-PS has distinct advantages over other conventional explosives for certain applications, particularly in small-scale manufacturing. The production methods are uniquely suited to micro-electromechanical systems (MEMS) type processing, leveraging a body of established techniques. The binary nature of the explosive can also ensure safety in manufacturing environments not equipped for energetics handling by facilitating the delay of oxidizer infiltration to later processing stages. These materials have been proposed for ignition devices and MEMS-scale fuzing where lower density compared to conventional energetics or explosives is not a critical factor and packaging can be engineered to control or exploit the apparent mechanical ignition sensitivity of e-PS [2]. Developing this technology could enable economical and repeatable igniters and initiators with a high level of microscale detail [3–6].

Material properties of PS can vary widely and may be tuned with etching conditions; however, studies on energetic applications have frequently used porosities around 60–70 % and pore sizes in the range of 2–15 nm which is

[a] *P. M. Guerieri, W. A. Churaman*
Sensors and Electron Devices Directorate
DEVCOM Army Research Laboratory
Adelphi, MD 20783, United States
*e-mail: philip.m.guerieri.civ@mail.mil
[b] *B. Fuchs*
DEVCOM Armaments Center
Picatinny Arsenal, NJ 07806, United States

termed ''mesoporous'' [7]. Galvanic etch conditions and properties surveyed relative to flame speeds by Piekiel et al. show the importance of high specific surface area (SSA), e.g., near 900 m^2/g [5]. Energetic performance can vary significantly by controlling PS material properties [5], composition of the solid oxidizer and its method of pore infiltration [8,9], environmental exposures or conditioning [8,10–12], and construction of MEMS-based superstructures like microscale channels [6]. This enables performance tuning, which along with MEMS-based manufacturing makes e-PS a flexible and economical system for precise design of repeatable explosive or pyrotechnic output in small form factors.

Combustion propagation rates observed for e-PS span several orders of magnitude from 0.1 to over 3500 m/s. This wide range suggests that different mechanisms of reaction propagation could be dominant depending on the properties of an e-PS composite, likely including conductive burning, convective burning, particle advection, crack propagation, and/or detonation-like shock coupling. Identification of dominant reaction mechanisms has been the topic of several past studies including some in which authors have debated which mechanisms give rise particularly to the highest e-PS propagation rates observed (exceeding 1 km/s) and whether such reactions constitute detonations [6,13].

By a simple qualitative definition, "a deflagration is a subsonic wave sustained by a chemical reaction and a detonation is a supersonic wave sustained by chemical reaction" [14]. Cooper defines detonation similarly as "a shock wave with a rapid exothermic chemical reaction occurring just behind the shock front" [15]. Most classical considerations of detonation theory treat the case of gaseous mixtures, but the same generalized Hugoniot relations apply to detonations in solid media, albeit solutions are more difficult since reliable equations of state are lacking at high pressures in relevant solids [14]. Velocity of the reactive wave is often used to classify a detonation versus deflagration. The latter is combustion supporting a subsonic wave, wherein the velocity is controlled by heat and mass transfer processes from one layer of flammable material to the next, processes that are much slower than the speed of sound in unreacted materials [14]. Detonation instead is the process by which a shockwave propagates through a flammable material, induces exothermic reaction by the drastic jump in temperature and pressure, and is sustained by the reactive energy release [14,15]. Qualitative differences between deflagrations and detonations in gases are given by Friedman and reproduced here in Table 1 illustrating the wide separations of their usual characteristics [16]. Since in most cases the utility of a detonating material is based on the significant associated pressure rise compared to the minimal pressure change in a deflagration, this distinction should be prioritized when attempting to classify reaction in novel types of energetic materials when their characteristics do not fall decisively on either side of this spectrum.

Table 1. Differences between Detonation and Deflagration in Gases, reproduced from [16].

Ratio[a]	Usual Magnitude of Ratio	
	Detonation	Deflagration
v_u/c_u	5–10	0.0001–0.03
v_b/v_u	0.4–0.7	4–16
P_b/P_u	13–55	0.98–0.99999996
T_b/T_u	8–21	4–16
ρ_b/ρ_u	1.4–2.6	0.06–0.25

[a] v = velocity, c = acoustic velocity, P = pressure, T = temperature, ρ = density. Subscripts: u = unburned, b = burned.

Since several processing controls can yield different e-PS composites with such widely varying reaction rates (and therefore significantly different controlling reaction mechanisms), this study limits discussion to PS/sodium perchlorate composites with typical linear flame speeds greater than 1 km/s, termed ''fast-burning e-PS". In this study, CHEETAH thermochemical calculations are performed that estimate detonation performance consistent with Chapman-Jouguet (CJ) theory. Empirical estimates for elastic properties including the speed of sound in PS [17–21], measurements of fast-burning e-PS propagation velocities from past studies [5,6,12,13], and performance of conventional primary explosives and nanothermites [22–29] are compared to the results of CHEETAH calculations to evaluate the feasibility of detonation to occur in reactions of fast-burning e-PS. It is proposed that while detonation feasibility varies with PS porosity, it is most likely to occur consistent with CJ theory at high PS porosities. At lower porosities, deflagration is more likely. However, the possibility of a unique type of detonation is also proposed at lower porosities wherein the 'detonation' velocity is slower than the speed of sound in downstream unreacted e-PS. This criteria precludes classical CJ detonation, but the unique composite nature of e-PS may allow a shockwave to survive at this sonic condition coupled to the reaction wave and thereby behaving in effect like a detonation. Rapid fracture of the PS nanostructure during an initial high pressure wave (termed herein a "precompression wave") ahead of the shock front could prevent complete decay of the shock energy forward into unreacted material.

2 Experimental Section

Thermochemical computations are made using the CHEETAH 9.0 code with the exp6.v9.0 library and several assumptions made to define compositions which emulate fast-burning e-PS [30]. Separate calculations are run at 0.5 % intervals of PS porosity between 45–85 % (void fraction before oxidizer infiltration). 69 % porosity is defined as the ''nominal'' case herein, being the mean of experimental test data between 56–80 % reported by Piekiel et al [5]. Fab-

rication by electrochemical etching in hydrofluoric acid results in hydrogen-terminated silicon on exposed surfaces, SiH_x (x = 1–3). This surface termination is an important and unique characteristic relative to other nanoscale metal/metalloid fuel candidates like aluminum which are frequently oxygen-passivated. For CHEETAH calculations the PS surfaces are assumed to be SiH_2 with a heat of formation of 274 kJ/mol [31] and density equal to that of elemental silicon (2.330 g/cm³) since density data for SiH_2 is unavailable and it represents surface termination on the silicon bulk crystal. Results are not significantly sensitive to changes in SiH_2 heat of formation and SiH_2 is not the major constituent. It should be noted however that the detonation performance computed is drastically diminished if the SiH_2 component is omitted. Brunauer Emmett Teller (BET) SSA measured by Piekiel et al. ranged from 191–475 m²/g and 581–901 m²/g for PS samples with average flame speeds below and above 1 km/s, respectively [5]. The average SSA of these fast-burning PS samples, 740 m²/g, is assumed for the nominal case of 69% porosity from which the SiH_2 mass fraction can be calculated. This computation is extrapolated across the range of 45–85% porosity by assuming the ratio of porosity to SSA is constant. (See Supporting Information for the results of CHEETAH calculations performed for each experimental data point reported by Piekiel et al in [5] using the reported porosity and SSA for each point.)

Sodium perchlorate is commonly used as the oxidizer to form a mixed binary fuel/oxidizer explosive. It is incorporated by drop-casting a saturated solution of sodium perchlorate in methanol onto the organophilic PS and allowing it to dry. Experimental estimates of pore-filling efficiency support the assumption made here that methanol solution completely fills the pores and evaporates, thereby precipitating the sodium perchlorate (i.e., 15.5% of pore volume is filled with sodium perchlorate oxidizer) [5]. The remaining pore volume is assumed to be filled with atmospheric air. The composition of the nominal case is provided in Table 2 and the mass fractions supplied to CHEETAH are plotted across the porosity range simulated in Figure 1. Entrapped air is important to include since most of the detonation products were expected to be in the condensed phase and the computations performed by CHEETAH rely heavily on the gaseous products.
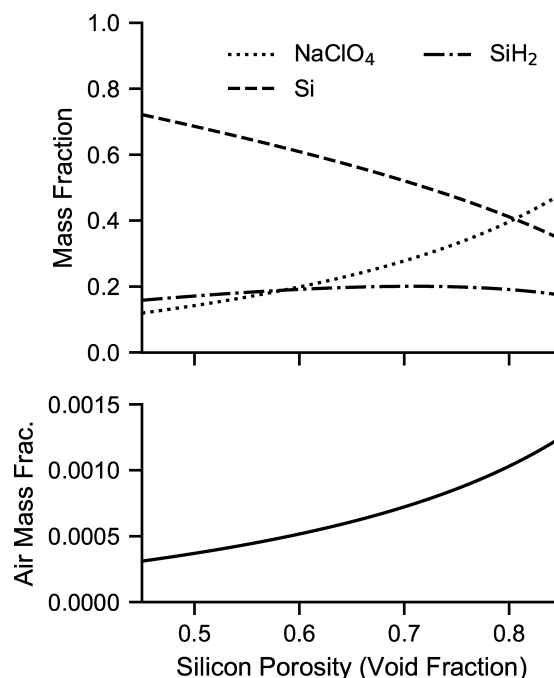

Figure 1. Formulation mass fractions calculated to simulate fast-burning energetic porous silicon composites as a function of PS porosity. (Top) Solid constituent mass fractions. (Bottom) Mass fraction of air.

3 Results and Discussion

3.1 CHEETAH Thermochemical Computations

The nominal formulation has an oxygen balance of −78.3% and mixture density of 0.989 g/cm³ or 41.5% of the theoretical maximum density (TMD). Figure 2 depicts the trade-off between increasing oxygen balance and decreasing density as PS porosity increases. The density penalty could be mitigated and oxygen balance improved by increasing the volume fill efficiency of the solid oxidizer to minimize the void space remaining in the composite, although effects on propagation rates and mechanisms would need to be evaluated. Generally all formulations are fuel-rich, which is limited by the geometry of the PS pores, oxygen density in the solid oxidizer, and pore filling efficiency. Porosities greater than 90% where stoichiometry can reach unity with this oxidizer system are not mechanically stable.

Properties of the CJ detonation state calculated for the nominal case are shown in Table 3 and plotted against PS porosity in Figure 3. Higher PS porosities correlate with improved detonation performance. This is expected since the PS pore volume available for oxidizer infiltration constrains the composite to fuel-rich mixtures. Higher porosities improve the oxygen balance, energy output, and performance. The actual detonation performance at low porosities is likely also overestimated by these calculations since non-ideal effects of the e-PS physical composite structure are
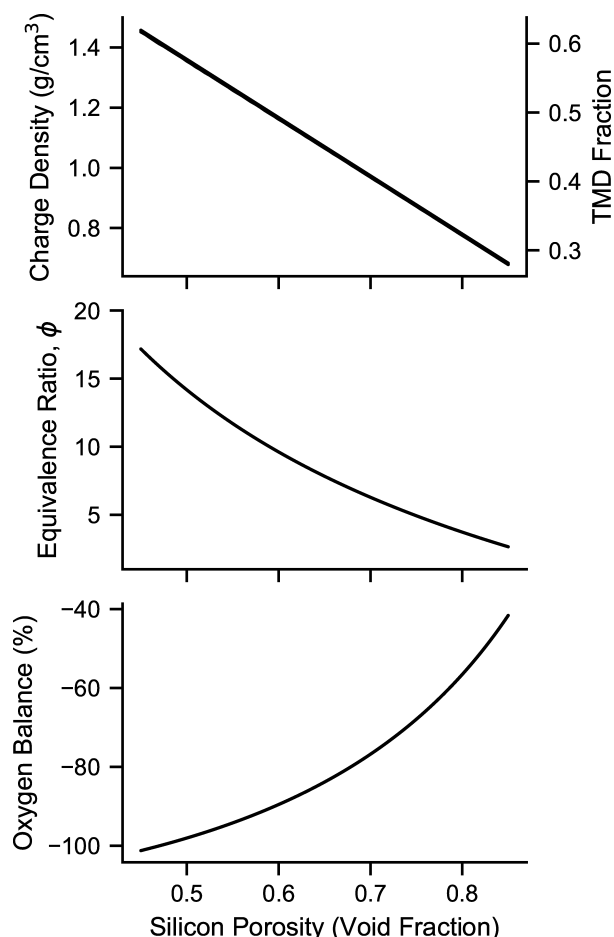
Table 2. Mass fractions of the porous silicon explosive formulation modeled in CHEETAH at 69% porosity.

	Si	SiH_2	H	$NaClO_4$	Air
Model Input (all H in SiH_2)	53.02	20.05		26.86	0.07
Si, H Element Balances (for illustration)	71.73		1.34	26.86	0.07

Figure 2. Formulation stoichiometry and density as functions of PS porosity.

Table 3. CHEETAH-calculated Chapman-Jouguet detonation properties at 69 % PS porosity.

Property	Value
Detonation Velocity [m/s]	1990
Particle Velocity [m/s]	557
Speed of Sound [m/s]	1430
Pressure [GPa]	1.07
Temperature [K]	3980
Detonation Energy, Gravimetric [kJ/g]	−5.89
Mechanical Energy, Gravimetric [kJ/g]	−1.87
Thermal Energy, Gravimetric [kJ/g]	−4.03
Detonation Energy, Gravimetric [TNT Equivalence]	1.32
Mechanical Energy, Gravimetric [TNT Equivalence]	0.429

not captured. CHEETAH computations are primarily driven by thermodynamic equilibrium of multiphase mixtures and CJ detonation theory. The calculations presented herein do not explicitly consider reaction rates limited by mass transfer due to structure. These assumptions are reasonable for fast-burning e-PS with extremely high SSA (ca. 900 m^2/g) and small nanoscale features infilled with oxidizer (pore

sizes ca. 3 nm) such that mass transfer is unlikely to be the dominant rate-limiter. This assumption weakens, however, as SSA decreases (which is assumed to vary linearly with PS porosity in these computations) and/or pore size increases such that diffusion could slow reaction rates, thereby departing from equilibrium. This is to say that CJ detonation theory, which assumes the detonation point is one of thermodynamic and chemical equilibrium, is unlikely to hold at low PS porosities where diffusion-limited reactions are significantly slowed and the CHEETAH-estimated detonation performance would be an overestimate. The computed performance may be better considered as an upper-bound. The same holds true for other cases in which the composite structure of the e-PS mixture could reduce reaction rates due to significant mass transfer effects, such as pore size being too small to allow effective oxidizer infiltration in the smallest pore branches.

Reaction products at the CJ state for the nominal case are shown in Table 4 and plotted across the range of porosities simulated in Figure 4. Most of the products are composed of molten silicon, with lesser but significant amounts of hydrogen gas, molten silica, solid sodium chloride, SiO vapor, and water vapor. The unreacted molten silicon is not contributing to the energy obtained from the detonation and decreases with increasing PS porosity as the oxygen balance improves. Increasing the pore-filling efficiency of the solid oxidizer (the ratio of oxidizer volume to available pore volume is currently estimated at 15 %) could lessen the liquid silicon products at all porosities.

Generally, less gas production is predicted than is typical of conventional explosives. Throughout the range of test data the detonation energy equivalence to TNT greatly exceeds the mechanical energy, i.e., thermal energy is significant. This is a result of the considerable condensed phase material produced such that little gaseous products are available to expand and perform mechanical work. In the nominal case, 7.54 mol/kg of gas are produced at the CJ point compared to 27.8 mol/kg calculated for TNT at 100 % TMD. Without gases to contribute mechanical energy, the low brisance of PS-based explosives would be relatively poor at breaking up and throwing surrounding materials, which is the basis of utility of most explosives. This limits, but does not eliminate, the manner in which these ex-

Table 4. CHEETAH-calculated products of detonation at the CJ state for 69 % PS porosity.

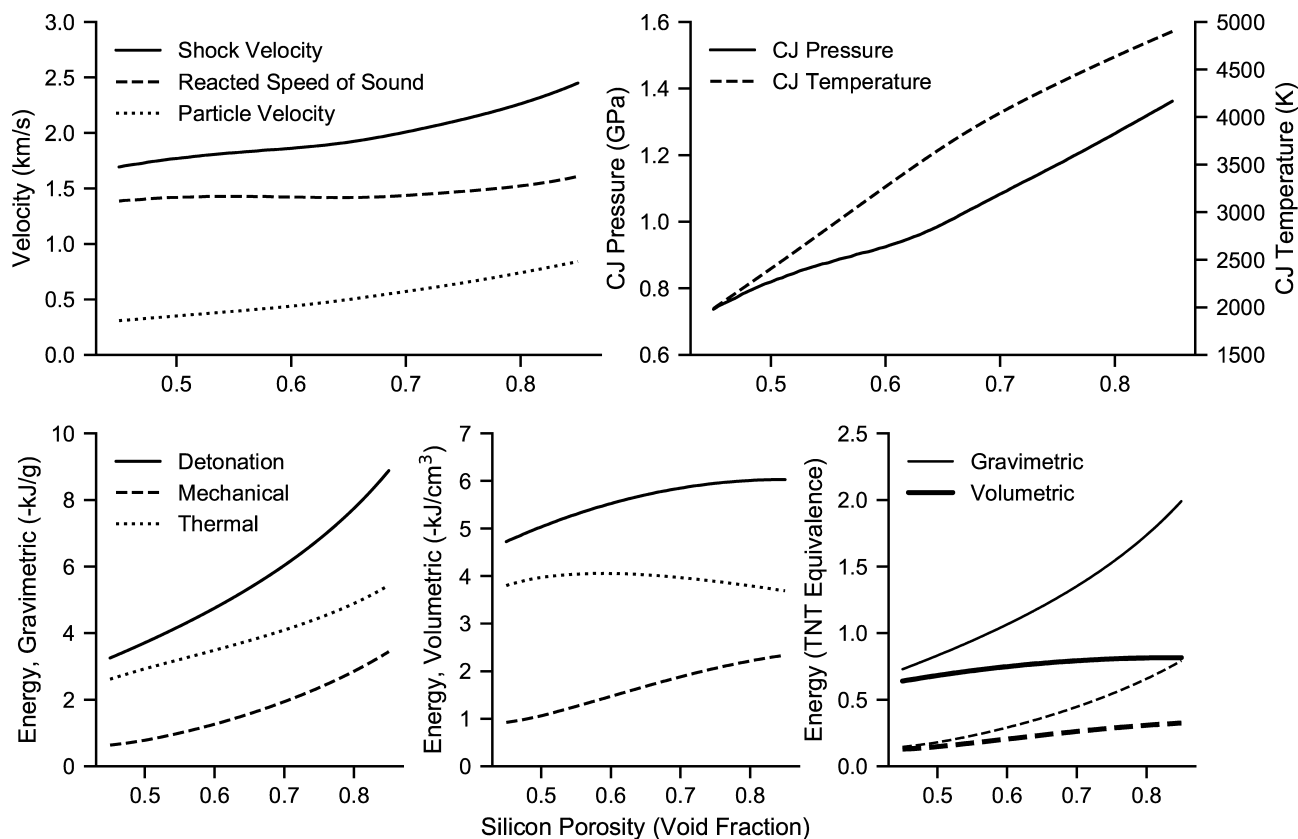| Product	Phase	Mass Fraction	Mole Fraction
Si	Liquid	0.593	0.613
SiO$_2$	Liquid	0.220	0.106
NaCl	Solid	0.124	0.062
H$_2$	Gas	0.012	0.168
SiO	Gas	0.031	0.021
H$_2$O	Gas	0.013	0.021
Total Gas		0.062	0.219
Total Condensed		0.938	0.781

Figure 3. CJ detonation performance calculated by CHEETAH 9.0 thermochemical code as functions of PS porosity from 45% to 85% void fraction. Calculation points spaced at 0.5% porosity intervals. Thermal energy in units of TNT equivalence is not calculated since the thermal energy from TNT is very small (< 0.1 kJ/g and kJ cm^{-3}), such that TNT-equivalent thermal energy is very large and of limited practical use. Therefore only detonation and mechanical energies are plotted as solid and dashed lines respectively in the plot of TNT equivalence.

plosives can be utilized, which could be useful for ignition and augmentation of initiator formulations. Gas production increases with porosity, particularly beyond ca. 70% above which the improving oxygen balance favors more SiO vapor products despite decreasing hydrogen gas production. Across all porosities, hydrogen gas is a major product due to dissociation of the hydrogen termination layer, which is known to occur at relatively low temperatures of 200–300 °C and could be of use for hydrogen storage [32]. The liberated hydrogen may also be better leveraged for explosive output if the oxygen balance can be improved to more efficiently tap the explosive potential of hydrogen.

Hugoniots of the detonation process computed by CHEETAH for three PS porosity cases (45%, 69%, and 85%) are shown in Figure 5. The CHEETAH predictions have a number of significant differences from those of more common detonating materials. As mentioned earlier, there is the very small percentage of gases formed while gas typically comprises the majority of the products of an explosive. Another major difference is the poor oxygen balance, −78.5%, limited by pore volume available for solid oxidizer infiltration. Most of the fuel does not react in the detonation reaction zone because of insufficient oxidizers. The

observed large flames emanating from the reaction are assumed to be the after-burn in air as hot silicon, SiO, and hydrogen are ejected. These two situations (prominent condensed phase products and highly fuel-rich oxygen balance) reduce the detonation pressure of the material. The CJ pressure of 1.07 GPa is much less than is typical for military explosives (25 GPa and above).

3.2 Elastic Properties of Porous Silicon

Information regarding the elastic properties of PS is limited and does not consider sodium perchlorate or other solids deposited within the pores [17–21]. It is also possible that variations of pore structure and size arising from different etch conditions and wafer properties affect the elastic behavior of the composite structures. Aliev et al. measured longitudinal acoustic (LA) velocity in PS films etched from P-type (boron doped) wafers of varying doping level and crystallographic direction and fit a semi-empirical expression for LA velocity in PS, where v_{0LA} is the longitudinal acoustic velocity in bulk silicon, ϕ is porosity, and κ is a fitting parameter [19]. Holding etch conditions constant (in-
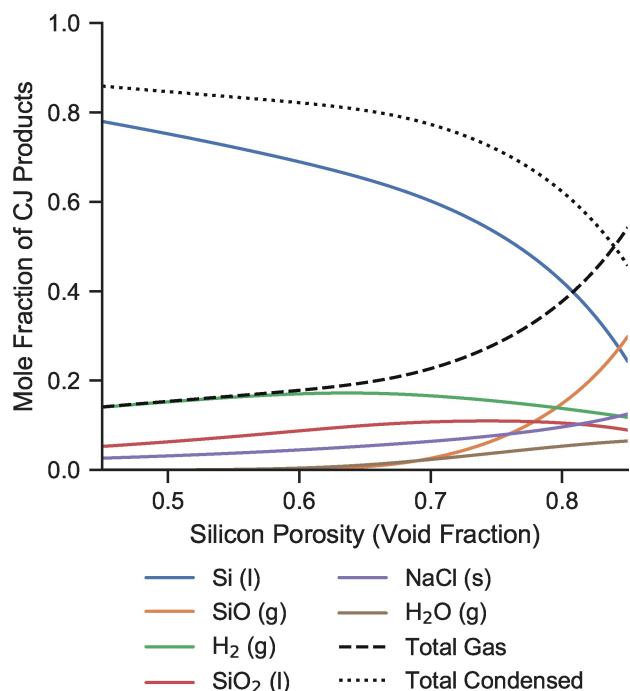
Figure 4. Reaction products at the CJ point calculated by CHEETAH 9.0 and total gas production as functions of PS porosity.
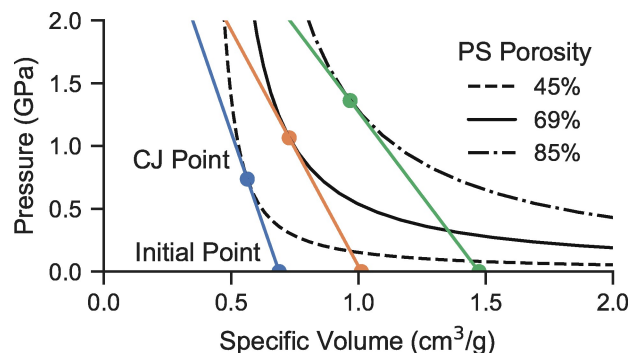

Figure 5. Detonation of porous silicon/sodium perchlorate. Calculated Hugoniots and respective Rayleigh lines for 45%, 69%, and 85% PS porosities.

cluding HF concentration and temperature), κ does not depend on crystallographic direction and varies with wafer resistivity according to an empirical relation [19]. For $R = 7.5\ \Omega$ cm, the estimated LA velocity in unreacted PS made from silicon wafers oriented in the [100] direction at 69% porosity is 1.73 km/s, lower than the detonation velocity calculated by CHEETAH at this porosity, 1.99 km/s.

$$v'_{LA} = v_{0LA}(1 - \phi)^{\kappa}$$

$$\kappa = 0.23 \log(R) + 1.15$$

Figure 6 depicts CHEETAH-computed CJ velocities and the LA velocity in unreacted PS according to this empirical fit with $\kappa = 1.351$. The shaded region represents the range of uncertainty in PS speed of sound contributed by variations in wafer resistivity between 6–9 Ω cm with the median line computed for 7.5 Ω cm. This speed of sound in unreacted PS crosses below the computed CJ detonation velocity at PS porosities above approximately 67% (65.7% to 71.0%). (This is very near the defined nominal porosity value of 69%, although there is no evidence that this is not coincidental.) It is notable that in general, energetic porous silicon is most commonly fabricated at porosities in the range of 60–70% [7], very near where the predicted detonation velocity and speed of sound are equal. This could be a source of stochastic results among different experiments since one velocity is not clearly dominant over the other.

In classical CJ theory, the explosive is shocked by the detonation wave, which causes chemical reaction that supports the leading shock. According to the theory, at the CJ point the detonation velocity is equal to the sum of the speed of sound (in the reacted material) and the particle velocity. Consequently, rarefactions behind the CJ point (i.e. after the detonation wave has passed) cannot overtake the detonation and cause its decay. The reaction zone of the shocked material lies between the shock front and the CJ point, isolated from external effects. This theory also assumes that the speed of sound plus the particle velocity in the reacted material at the CJ point exceeds the sound speed of the unreacted material ahead of the shock front, otherwise a shock cannot be sustained since the acoustic energy will propagate forward of it at the unreacted speed of sound. In the case of e-PS however, the predicted deto-
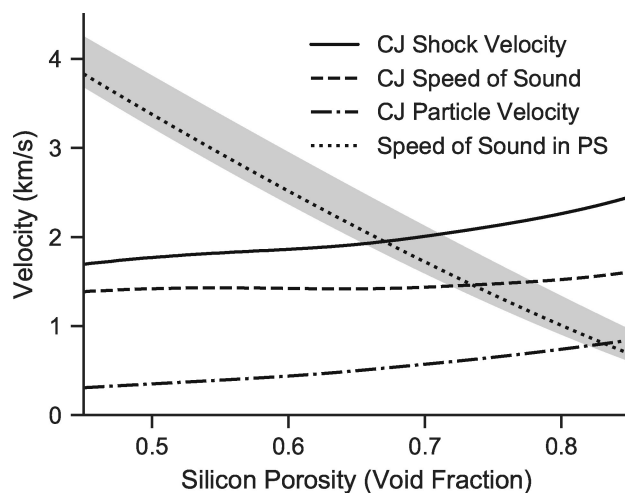

Figure 6. CJ velocities computed by CHEETAH and resistivity-dependent longitudinal acoustic velocity in 6–9 Ω cm porous silicon from Aliev et al. [19] represented by shaded region and median line computed for 7.5 Ω cm. PS speed of sound also estimated assuming that the infilled oxidizer decreases the porosity to offer an upper bound on the speed of sound in e-PS composite.

nation velocity only exceeds the unreacted speed of sound at PS porosities exceeding 67%. At such high porosities, a detonation consistent with classic CJ theory is predicted by these simulation results.

It appears unique that at PS porosities below 74% the unreacted sound speed exceeds the reacted material sound speed. In contrast, the reaction products of a traditional high explosive usually have greater sound speed than the unreacted materials since the products are at a higher density and much greater temperature.

Still lower, at PS porosities below 67%, the unreacted PS speed of sound also exceeds the CHEETAH-calculated detonation velocity, disagreeing with CJ theory. In this low porosity range, deflagration controlled by advection and convection (possibly with crack propagation) is most likely since the reaction propagation speed would lie below the unreacted speed of sound (i.e. it is subsonic) [13]. This conventional classification however assumes that the unreacted material into which the deflagration propagates has not been affected in such a way as to change its sound speed. I.e. this is based on the unreacted speed of sound being the 'local' speed of sound of the reactive wave, by which its sonic mach number can be applied (and is less than one).

It is therefore worth considering whether conditions are feasible in which the unreacted material could be affected by an incipient or approaching reactive wave in such a way that its sound speed is quickly reduced. If this occurs before the majority of the reaction wave arrives, could the mach number of the propagation be better assigned by the sound speed of this 'affected' material such that the overall propagation is (while inconsistent with CJ theory) 'detonation-like'? While conventional deflagration mechanics (and Occam's razor) suggests this situation is less likely, it cannot yet be ruled impossible.

Considering the feasibility of this scenario, particularly in the transition zone of PS porosity just below 67%, a sonic wave would need to precede any detonation wave as initial energy of reaction reaches unreacted material and propagates at the unreacted sound speed, termed herein a "precompression" wave. Further consideration of ePS elastic properties is required to assess whether rapid decrease of the unreacted speed of sound is possible due to stimuli of such a precompression wave.

Dynamic strain response of non-porous silicon remains an active area of research. The Hugoniot elastic limit (HEL) is the stress level at which the material response transitions from an elastic strain response to elastic-plastic. Silicon has a high HEL of 5–9.2 GPa depending on crystal orientation [33–35], so the CJ detonation pressure is well below the HEL of solid silicon. High variable strain rate compression experiments on single crystal silicon by Smith et al. showed that peak stress can exceed twice the HEL, up to approximately 20 GPa, within 100 μm of the loading surface (11.7 ns) in the [100] direction before relaxing to the HEL.

Relaxation in the [110] and [111] directions is about 100 times slower (out to ~10 mm in >1 μs).

However, data is limited that describes compressive yield stress of silicon which is porous (PS) as a function of porosity or etching parameters [36–39] and no experimental studies on the high-strain rate response of PS to shock loading are available. Lane et al. have considered this problem using molecular dynamics simulations in LAMMPS to study a shock driven into a silicon domain with porosity [17–18]. Their simulation results suggest that silicon undergoes enhanced densification under shock loading when the porosity is introduced, reaching higher density at given elevated pressures than does fully dense silicon at the same pressure. The elastic-plastic Hugoniot region shifts to lower pressures and densities (higher specific volumes). This is attributed to local solid-solid phase change near the voids to a β-tin phase. As the shock front reaches ambient material, shear stress is maximum in a region of shocked elastic response before being relieved by the phase transformations in a "mixed final state of partially transformed material and elastically compressed diamond cubic phase" [18]. From this maximum shear stress, Lane et al. computed a so-called dynamic strength value for several simulation cases at 0%, 5%, 25%, and 50% porosity and fit it to a function of porosity, ϕ, $Y = 10e^{-5\phi}$ GPa. Although not stated as such, this dynamic strength is similar to a HEL where the PS material response transitions from elastic to elastic-plastic. The fit of this dynamic strength crosses 0% porosity at 10 GPa, near the HEL of silicon.

Klyshko et al. fabricated tensile test structures in PS films on p+ 0.01 Ω cm PS wafers in the [100] direction by adhering Cu to the topside and etching a meniscus shape in the PS profile with KOH solution. Breaking strength was fit to the empirical function of porosity, $\sigma = \sigma_0(1 - \phi)^m$ where σ_0 is the ultimate strength of bulk silicon and the fitting parameter, m = 2 [37]. Higher wafer doping was used relative to 6–9 Ω cm PS considered here, the effect of test structure fabrication methods on the PS strength is poorly understood, and the bulk Si breaking strength used for the fit was not provided. Nevertheless, assuming an ultimate tensile strength for silicon of 0.17 GPa and that the ratio of compressive to tensile strength of bulk silicon is 1:18 leads to a compressive strength estimate for PS at 69% porosity of 0.3 GPa, or about one fourth of the CJ pressure of 1.07 GPa. Figure 7 compares both the dynamic strength fit from MD simulations of Lane et al. and the compressive strength estimate based on Klyshko et al. to the estimated CJ pressure across the porosity range. Notably, these two estimates of PS strength agree closely in this porosity range. The detonation pressure predicted is seen to exceed the material strength at PS porosities greater than 50%.

Returning to the question of whether it is feasible that a precompression wave could reduce the unreacted material speed of sound (especially just below 67% PS porosity), this approximated relation of PS strength to detonation pressure is important. The amplitude of the sonic precompression wave
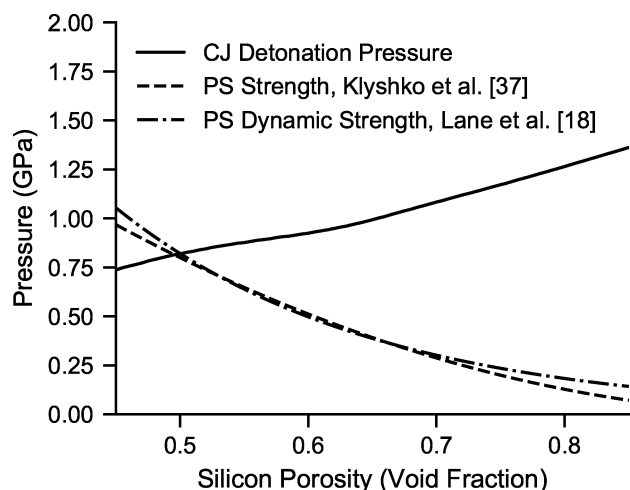
Figure 7. CHEETAH calculated detonation pressure relative to estimated PS compressive strength based on Klyshko et al. tension tests [37] and Lane et al. MD simulations [18].

predicted in this porosity range could cause material failure in the PS when exceeding the material strength. For example, at 65% porosity, the CJ detonation pressure predicted is more than twice the estimated material strength. As e-PS initially deflagrates, it could run up in reaction pressure as high as the material strength (~400 MPa) before it causes mechanical failure. Once this occurs, the unreacted speed of sound estimates for PS are no longer valid and presumably with lower interconnectivity of the silicon matrix, the sound speed would be lower once the foam-like network catastrophically fails. If ample energy is available from chemical reaction behind this fracture plane to drive the reaction front faster than this local 'fractured-PS speed of sound', then a shockwave could form at the reaction front with high-pressure unreacted (but disintegrated) e-PS ahead of the front. Since the speed of sound local to the shock and reactive wave is lower than the shock velocity, it would constitute a detonation, albeit atypical in structure. Some energy dissipation forward of the detonation wave would be expected perpetually as the fracture plane continues to propagate with the detonation. If fracture ceases, the detonation wave would decay into the precompression wave until rapid fracture begins again, possibly with a cyclical or repeated nature. This could contribute some stochastic behavior to the propagation velocity and amplitude of precompression waves ahead of the reaction front. It is worth noting that it is unknown whether the initial run-up in reaction pressure to 400 MPa with a deflagrating reaction front is possible. Otherwise an initial small-scale input shock may suffice to contribute the initial structure for this fracture plane mechanism to form.

Considering more generally: these aforementioned conditions exist for PS porosities between 50% and 67% where the CJ pressure exceeds the estimated PS material strength. Acoustic energy transfer in the sonic precompression wave forward of the shock front could be limited by PS mechan-

ical failure, despite the unreacted material sound speed being greater than the reactive wave speed. In this dissipative mechanism, the fracturing could prevent efficient energy transfer from a shockwave at the reactive front to the forward precompression wave such that the shock wave does not decay (i.e. decreased sound speed in the fractured layer of PS ahead of the reactive wave makes it supersonic and can support a stable shockwave).

Therefore, even though the classical criteria for detonation is violated in this low porosity range, with propagation being subsonic relative to the sound speed in unreacted material, the rapid fracture of the porous network to a lower sound-speed material offers a plausible means by which a shockwave could be prevented from decaying and sustained by reaction immediately following it.

At PS porosities just slightly less than 67%, the precompression wave propagating at the speed of sound in the unreacted material would be only marginally faster than the detonation wave. Strength would be exceeded by the CJ pressure by a factor of three. Therefore this proposed dissipative detonation structure is most feasible at these porosities. Closer to 50% porosity, the precompression wave would be significantly faster than the detonation wave and the predicted CJ pressure is nearly equal to the material strength, so decay of the detonation front would be far more likely and the proposed dissipative detonation structure is least feasible here. A transition is therefore predicted to exist somewhere between 50% and 67% PS porosity, under which detonation would cease to occur because a shock wave cannot be sustained. The feasibility of this dissipative detonation type in the transition zone between classical CJ detonations likely at higher e-PS porosities and convective burning in low-SSA slow-burning e-PS is further supported qualitatively by considering the criteria in Table 1 relative to CHEETAH-predicted performance. With a Mach number of 0.5–2, significant pressure rise predicted, and enhanced densification of PS, e-PS is positioned firmly between a conventional detonation and deflagration. Ultimately a classification may be academic and will surely in itself fail to affect performance and therefore appropriate use cases of e-PS. However, significant pressure rise alone, pending further experimental verification, would align possible uses with those of detonating explosives, albeit in niche cases when the relatively poor performance compared to modern high explosives is allowable.

3.3 Comparison to Test Data and Flame Jump Observations

Reaction propagation of e-PS has been examined by several groups using strips of e-PS confined on three sides by the parent silicon wafer substrate. Fabricated on semiconductor wafers, most test articles are tens of μm thick with mm to cm in-plane dimensions. Discontinuous flame jumps are occasionally observed in the fastest-burning varieties of e-PS

P. M. Guerieri, B. Fuchs, W. A. Churaman

characterized by discrete downstream ignition points ahead of the reactive wave front from which a new luminous front propagates. Figure 8 shows examples of flame jump events observed by Piekiel et al. [6] and Plummer et al. [40]. These flame jumps complicate measurements of reaction velocities especially when high-speed video of the luminous front is used, and may cause overestimation of flame speeds if overall time of arrival is used to estimate steady propagation rates (since flame jumps cause unsteady propagation). Therefore, it is important to define specific nomenclature to classify the types of velocity measurements in e-PS reactions. Herein, "flame speed" denotes velocity of a steady luminous front observed without flame jump discontinuities, "jump speed" denotes velocity between two discrete ignition points (which may include the original source ignition), and "reaction speed" denotes a resultant velocity from an ignition point to arrival at a certain datum location including any steady flame propagation and discontinuous flame jumps that occurred within that region. When the type of velocity measurement cannot be clearly identified, it is assumed to be a reaction speed. Figure 9 provides a hypothetical graphical representation of these definitions. Piekiel et al. theorized for rapid combustion (> 1,500 m/s) that flame jumps may be caused by acoustic or shock events traveling through the porous film [6].

Reaction propagation rate data from four studies of fast-burning e-PS (PS + NaClO$_4$) composites are plotted in Figure 10 with the CHEETAH-computed detonation velocity and estimated speed of sound in unreacted PS (1–10 Ω cm) according to Aliev et al [19]. A second calculation of sound speed in unreacted PS is also drawn by assuming the in-filled oxidizer decreases the porosity as if it was additional silicon. While this is likely an overestimation, it is meant to be an upper bound on the sound speed of unreacted composite structure since the additional solid oxidizer is not considered in the semi-empirical estimate from Aliev et al.. Piekiel et al. estimated jump velocities and originally noted the close match to PS sound speeds, which is also evident in Figure 10 [6]. The jumps are also only reported below 67 % porosity where the unreacted sound speed is estimated to exceed the detonation velocity and a pre-compression wave would be expected ahead of the detonation wave. This is possibly a result of unintentional artificial selection of the independent variables of etch conditions and further investigation to specifically survey for flame jumps observable above 67 % porosity would be valuable. Nonetheless, it is thought that the sonic pre-compression wave preceding the detonation/reactive wave impacts a structurally weak location, causing breakage and initiation seen as a flame jump. It is known that e-PS can be sensitive to ignition by contact and PS fracture (and extreme caution should be exercised in any experimental procedure). It is unknown what defects or structural features may cause this effect and it is possible that the ignition delay associated with each discrete downstream ignition is variable. Therefore their timing could vary between the
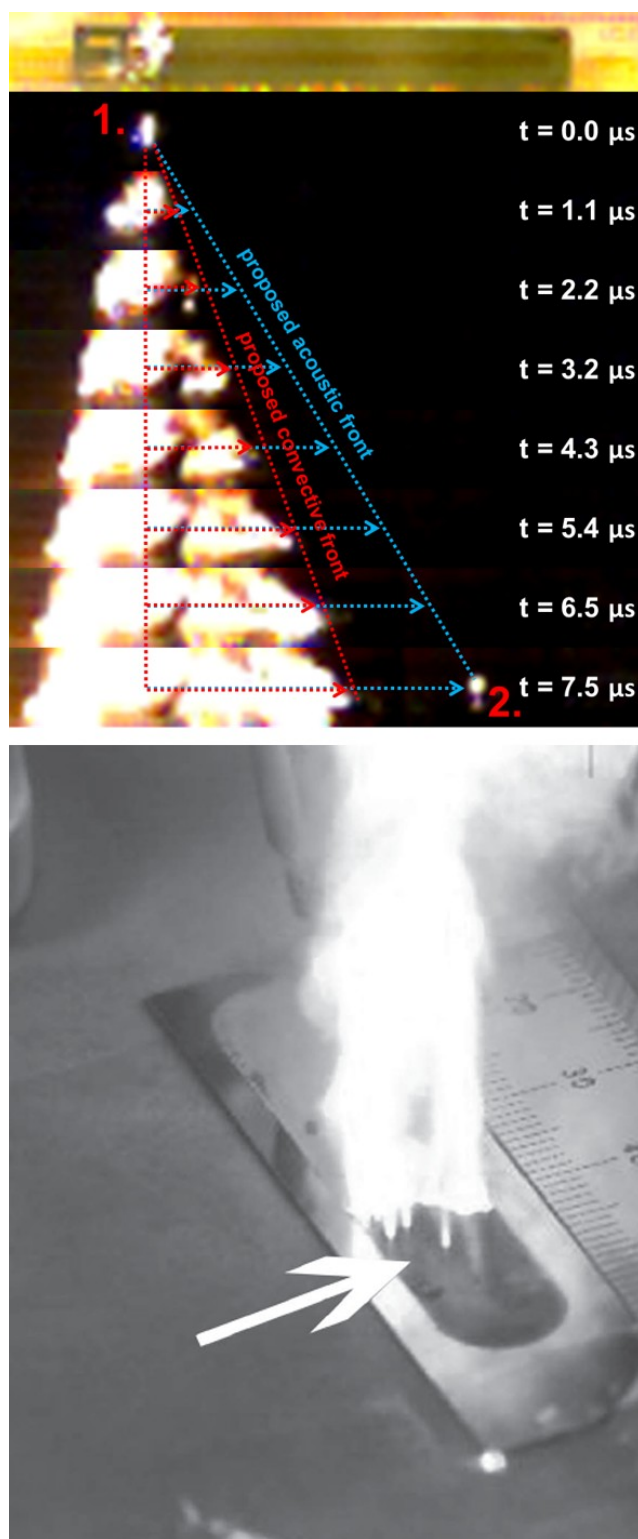

Figure 8. On-Chip PS flame jump examples. (a) Jump visible at 7.5 μs reproduced from [6]. Following the nomenclature of Figure 9, the annotated "convective front" would be a flame speed and proposed "acoustic front" a jump speed. (b) Flame jumps shown by arrow reproduced from [40].
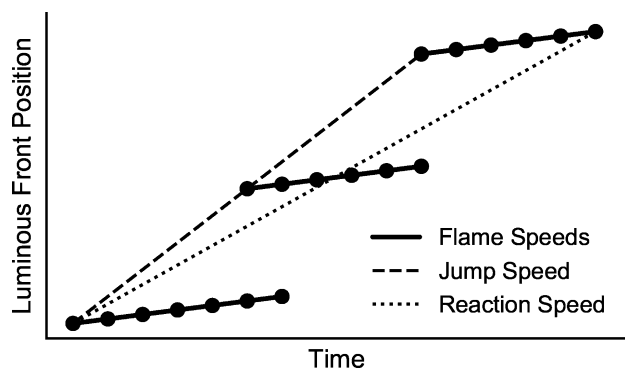
Figure 9. Hypothetical graphical representation of nomenclature defined for velocity measurements of PS combustion propagations with two flame jumps.

constraints of the faster acoustic velocity of the precompression wave and the slower detonation velocity carrying the main reaction front, which is consistent with published experimental results shown in Figure 10.

Furthermore, as discussed above, with decreasing porosity the strength of PS increases while the detonation pressure decreases, so the ability of a precompression wave to break PS will weaken and flame jumps would be expected to cease at some PS porosity between 50–67%. No experimental jump velocities were reported by Piekiel et al. below 59%. It is suggested that the "proposed acoustic wave" moving ahead of the "proposed convective front" denoted by Piekiel et al. reproduced in Figure 8 represents the predicted sonic precompression wave moving ahead of a detonation wave, respectively.

Several reported flame speeds approach or match the CHEETAH-estimated detonation velocity without exceeding it and represent possible detonations [5, 6, 12]. Piekiel et al. completed a survey of reaction speeds resulting from PS made with different combinations of wafer resistivity and HF etchant concentration and several of the proposed detonation examples are derived from two experimental data sets from that study: 1–10 Ω cm wafers and > 30 Ω cm wafers with PS porosity varied using HF concentration [5]. The inset of Figure 10 replots the experimental reaction veloc-
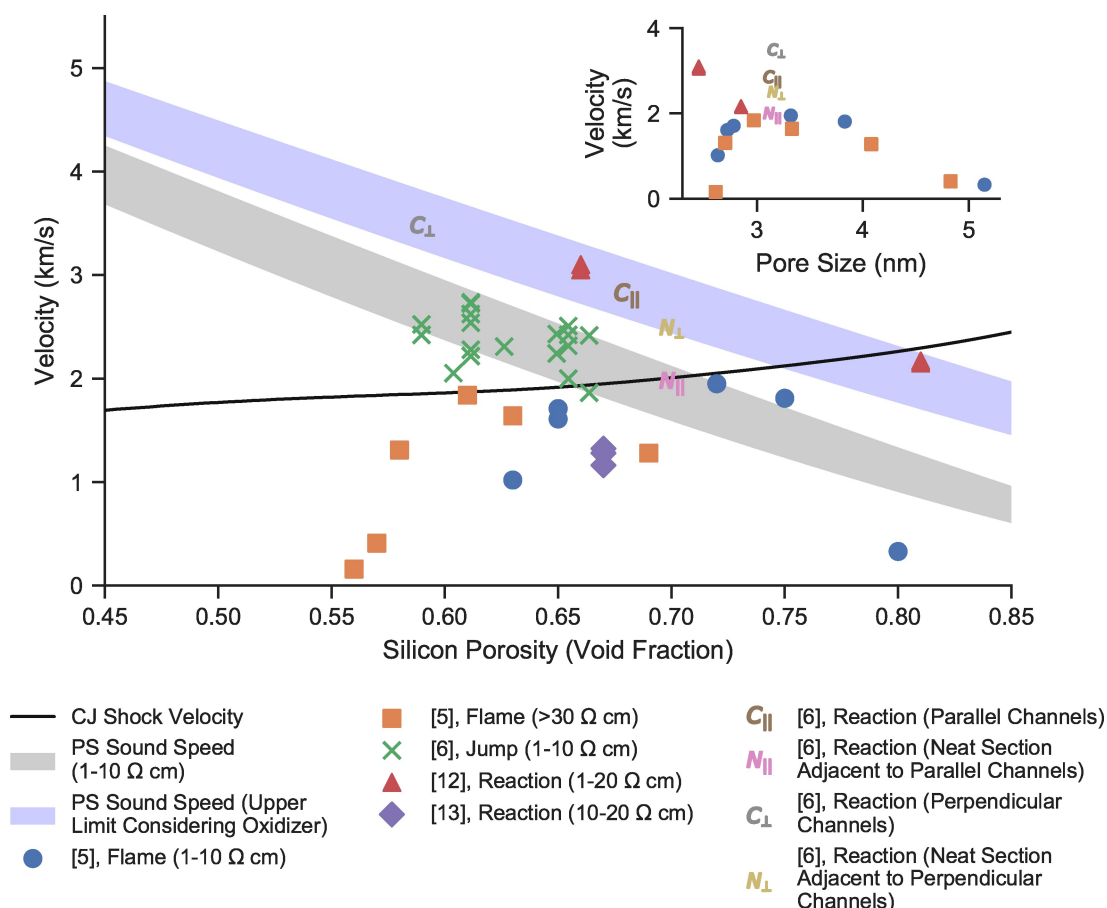

Figure 10. Comparison of CHEETAH-computed CJ velocity and speeds of sound estimates in PS with experimental observations of reaction and jump velocities in fast-burning e-PS [5, 6, 12, 13]. Note that channelled samples tested by Piekiel et al. are plotted against their 'artificial' calculated porosity which accounts for additional void space of the open channels [6].

ities versus pore size if available and it can be seen that both of these data sets from Piekiel et al. [5] directly overlap and reaction velocity drops quickly at pore sizes smaller than 2.75 nm and (more gradually at) larger than 4 nm. It is near the peak of this curve at approximately 3 nm that the reaction velocities are consistent with the CHEETAH-computed detonation velocities. CHEETAH runs were also completed with reactant mass fractions recalculated based on the porosity and SSA reported for each of these data points from Piekiel et al. (otherwise in this study, SSA is assumed to scale linearly with porosity). Results of these calculations along with tabulation of the error (overestimation) of the CHEETAH-calculation detonation velocity compared to the experimental observation are shown in Supporting Information. Notably, a plot of these errors versus pore size matches the trend seen in the inset of Figure 10. The minimum error is observed at 3 nm. Pore size in e-PS composite explosives therefore appears to be critical for e-PS reactions in practice to be consistent with CHEETAH-predicted detonation performance. As discussed previously, this deviation of practical performance from prediction with pore size could be explained by increasing mass diffusion distances for elementary reactions with increasing pore size, and incomplete or inhomogenous pore filling with oxidizer at small pore sizes. There may also be additional variations or nonidealities, e.g., abnormal or spatially varying pore structure, more varied surface termination chemical groups, or incomplete oxidizer inclusion, which could preclude or modify conditions for detonation and introduce scatter in both experimental velocities and porosities.

Parimi et al. reported average "reactive wave propagation speeds" of 62–67% porosity PS in air at 0.1 MPa, air at 0.01 MPa, and helium at 0.1 MPa, concluding that consistency among tests in these environmental conditions shows that gas-phase acoustics do not affect the propagation, which is instead governed by mechanisms within the condensed phase [13]. The conclusion that the condensed-phase acoustics are critical is consistent with the mechanism proposed herein based on the CHEETAH computations. However, Parimi et al. also conclude that since the reaction speed is below the unreacted PS sound speed, they are not detonations. This is supported for the specific samples in the study by measurement of sound speed in the PS with microechography which exceeds the observed reactive wave speeds. The reactive wave speeds do fall below observations of Piekiel at 65% porosity by approximately 0.5 km/s and the pore size is not reported, which could have deviated from the ideal size near 3 nm. Computation results presented here instead show an opposite relation of sound speed and reaction velocities at PS porosities >67%, where the predicted reactive wave speed (and that of several experimental observations) exceeds the unreacted e-PS speed of sound. In this range, a classical detonation structure is feasible and the conclusion by Parimi that their samples did not detonate cannot be categorically applied to the e-PS system overall. Furthermore, at lower

porosities where this velocity relation given by Parimi et al. is valid, it only suggests that a precompression wave exists and does not outright preclude a shockwave sustained by rapid fracture of the PS structure as described previously. A weakened detonation of this fashion is consistent with some lower experimental velocities compared to the CHEETAH detonation speeds at PS porosities less than 70%. It is also likely that cases exist in which enough energy propagates downstream in the sonic precompression wave, or in which non-ideal structures of the e-PS composite cause significant mass-diffusion limits on the reaction rate, such that a detonation shockwave cannot be sustained. Such situations are consistent with the conclusions of Parimi et al. Nonetheless, future experimental measurements of pressure during reaction would offer valuable insight into the pressure rise associated with the reactive wave, whether they are sufficient to be termed detonations, and which critical factors affect the pressure rise generated.

Lastly, four experimental propagation velocities exceed both the CHEETAH detonation velocity and the estimated unreacted PS sound speed. Data from Becker et al. at 66% porosity is the only observation for typical unaltered PS (i.e., without additional microscale superstructure) and is a high outlier that may be affected by the unique velocity measurement technique that used patterned surface bridge resistors along the sample length [12]. Although the measurements were supported by high-speed video, this flame speed has not been replicated since. The other three aforementioned observations resulted from test samples fabricated by Piekiel et al. where 50 μm channels were cut in the silicon substrate before etching PS 20 μm thick [6]. Although all PS fabricated in these samples was 70% porous, an artificial porosity was computed for channeled cases to include a penalty for the empty space of the channels (and the observations are plotted against these artificial porosities). The samples also included three sections of the PS on each strip that alternated between channeled and unaltered PS, or vice versa. Velocity of both perpendicular and parallel channelled sections exceed the CJ detonation velocity and unreacted PS sound speed, but are very similar to the upper limit of unreacted PS-composite sound speed represented by reducing porosity in the Aliev et al. calculation for infilled oxidizer. Stress concentrations near channel corners may contribute to the mechanism of precompression waves causing flame jumps. If this occurs continuously enough, it could manifest as an inflated reaction speed consistent with the channeled section observations. The last data point that propagates faster than predicted is an unaltered PS section that was situated between two perpendicularly channeled sections, which could have been influenced by strong initial shock energy from reaction of the first channeled section.

3.4 Comparison to Nanothermites and Primary Explosives

Formulations of e-PS are similar to nanothermites, in which nanoscale metal powder fuels are mixed with solid oxidizers to form a fast-reacting bi-component energetic (silicon nanoparticles can be used to formulate Si-based nanothermites). A difference is that PS is foam-like and derives its high SSA from internal structure of connected pores, whereas nanopowders derive surface area from the outer surfaces of independent nanoscale particles (which are frequently agglomerated or in composite-bound superstructures). PS can be imagined as a highly connected and stabilized nanoparticle bed with passivation on only the exposed surfaces and all crystal lattices of the particles aligned. This higher connectivity of the fuel in e-PS relative to particulate nanothermite fuels opens the possibility of new mechanisms by which hydrodynamic strains on the order of the charge diameter can propagate within and interact with the pore network structure of the fuel. Carbon materials can form similar nanoporous materials and a recent report was made of possible detonation observed in a composite of functionalized carbon black with sodium perchlorate infilling the pores [41].

Khasainov et al. recently evaluated the potential of nanothermites to replace primary explosives for initiation or ignition [22]. The review considered combustion mechanics of fast-reacting nanothermites (flame speeds exceeding 500 m/s) with respect to baseline primary explosives, lead azide and mercury fulminate, concluding that state-of-the-art nanothermites still do not compare to primary explosives in terms of triggering capability. Despite nanothermite reaction propagation rates observed up to 2.5 km/s [23,24] and some claims that these reactions are detonations [23–26], Khasainov et al. argue that nanothermite combustion is controlled by convective heat and mass transfer and do not constitute detonations led by a steadily coupled reaction wave and shock front. This is supported by examples of nanothermite formulations with significant gas generation [23,24,27], which would enhance convective transfer, that also feature higher flame speeds. In addition, the highest nanothermite flame speeds are observed for very low density samples at 3–20% TMD, ca. 0.8 g/cm^3 and increasing their charge density drastically reduces the flame speeds [28,29], further supporting a convective mechanism that is more efficient at low density. Measurements of pressure within reacting nanothermites are limited but available data show compressive pressure wave amplitudes only as high as 20 MPa [26,28], 2–3 orders of magnitude lower than that of high explosives [22].

In the case of e-PS, however, the reactive mechanism is less likely to be exclusively convective. The CHEETAH-calculated reaction products are less than 6% gas by mass in the nominal formulation case, in contrast to strong gas generation in fast-reacting nanothermites such as Al/Bi$_2$O$_3$ or Al/I$_2$O$_5$ which can react at temperatures exceeding the boiling points of bismuth and iodine [22]. e-PS can also exhibit

fast reaction propagation above 1 km/s at higher densities than nanothermites, up to 51% TMD (e.g., 1.31 km/s observed flame speed at 58% PS porosity, 1.21 km/s estimated density [5]) and increasing density does not correlate with strongly decreasing flame speed across all PS porosities [5]. Figure 11 shows plots of CJ pressure and detonation velocity estimated by CHEETAH for e-PS compared to fits of experimental data for lead azide and mercury fulminate [22]. Both CJ pressure and detonation velocity of e-PS decrease with increasing density, consistent with nanothermites, but this correlation is weak and can also be explained by worsening oxygen balance as shown in Figure 2. Similar to nanothermites, e-PS performance is weakest compared to primary explosives at high densities. Contrary to present arguments for convective burning precluding detonation in nanothermites, e-PS experimental flame speeds in relation to density and CHEETAH-calculated performance
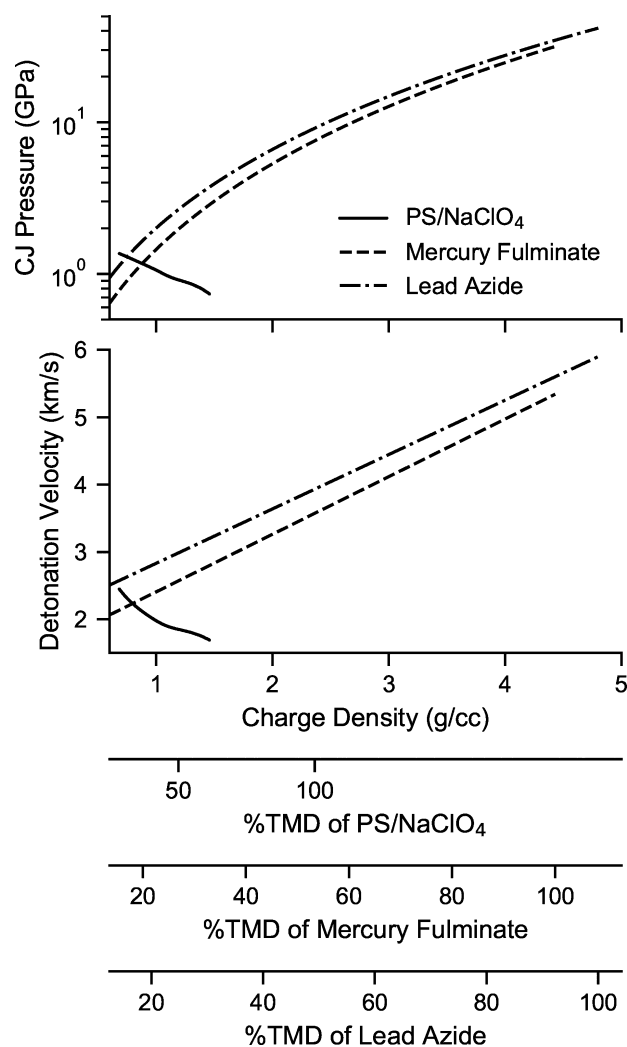
Figure 11. Comparison of CHEETAH-estimated e-PS (PS+NaClO$_4$) detonation velocity and CJ pressure to fits for primary explosives from [22].

suggest that detonation is feasible and performance characterized by CJ pressure could be within one order of magnitude lower than primary explosives. Nanothermites reaction pressure is at most 2–3 orders of magnitude lower than primary explosives. Therefore, e-PS is a more viable replacement or augmenting component for small charge size primary explosives in terms of initiation potential than granular nanothermites and constitutes the closest a metal/metalloid-based bi-component energetic has come to a detonable explosive at size scales relevant to igniter devices.

3.5 Discussion of Reaction Mechanisms

Fast-propagating e-PS, referring here to porous silicon infilled with sodium perchlorate oxidizer with reaction propagation rates exceeding 1 km/s, is set apart from conventional explosives and micro- or nanoscale metal-based particle composite reactive materials by its single-crystal porous superstructure, extremely small (ca. 3 nm) composite mixing length scale, metastable hydrogen termination in lieu of a passivation layer, and the low-gas production expected from its reaction. Parimi presented a thorough consideration of conduction and convection mechanisms in e-PS evaluating whether they could account for extreme differences observed in the propagation rates of slow (ca. 1 m/s) versus fast (ca. 1000 m/s) propagating e-PS [42]. Enhanced thermal diffusivity of silicon promoting the rate of conductive transfer compared to nanothermites and explosives was shown to fall short of accounting for the higher propagation rates observed by an order of magnitude. Differential scanning calorimetry by Parimi also highlighted the decrease in activation energy between the different e-PS types, but it was noted that repeating this analysis at high heating rates could improve its accuracy. Parimi also justified that regarding a convective mechanism, structured e-PS would not permit dispersion of unreacted material identified in particulate nanothermites by Densmore et al. [43], and the small pore sizes in e-PS would significantly limit convective downstream gas permeation. The analysis of Parimi highlights the possibility that the high e-PS propagation rates could instead be fast deflagrations driven by a combination of enhanced conduction, reduced activation energy, and so-called PS-specific mechanisms enabled by unique properties of the material, namely crack propagation. While further consideration of the role of crack propagation in e-PS reaction is warranted, Viljoen and Hlavacek noted that crack propagation is typically observed at 50–65% of the speed of sound in an isotropic solid and is therefore not expected to contribute to supersonic combustion (although superposition of it with deflagration can add instability that promotes transition to detonation) [44]. When detonation does not occur in e-PS reaction, it is likely to at minimum be controlled by the confluence of these factors culminating in a fast deflagration with lower re-

sultant pressure, especially given the low-gas production expected. Distinguishing fast deflagration from detonations in the e-PS system therefore remains an experimental challenge, likely with significant implications on its potential uses if the distinction is based on varying peak pressures realized. The fine delineation of the two in this system could also be a means of engineering one or the other with small changes in reactive composite properties.

Low gas production however also does not preclude detonation as demonstrated by gas-gun, wedge test, and CHEETAH calculations by Davis et al. on Ti/PTFE and Al/Fe_2O_3/PTFE reactive systems which indicated that detonation-like phenomena can be observed in agreement with CHEETAH results [45]. Davis et al. note that, as opposed to standard explosives which can start reacting by decomposition of a single crystal, pure metal/metal or metal/metal oxide reactive materials need interaction of the constituents for chemistry to occur, i.e. by diffusion and during melt. But when adding the fluorinated polymer in their study, the reaction threshold is lower because the polymer can decompose and initiate reaction with remaining reactants. This is notably similar to e-PS in which the hydrogen termination layer contributes a significant constituent which is known to dissociate to hydrogen at low temperatures. Similar to the aforementioned fluorinated polymer decomposition, hydrogen dissociation can further the reaction with and between silicon and the oxidizer. In both cases, these offer a mechanism by which a propagating shock can cause rapid reaction consistent with detonation structure.

Additional consideration of the e-PS system with respect to theory of detonation structures specific to very porous charges would be valuable, especially in the moderate porosity regime near 67%. The precompression wave proposed herein to precede the detonation shock front would dissipate at least some energy from the detonation (even if material disintegration limits the energy transfer), and the classic ZND model would not be strictly applicable. In a review on steady detonation Fickett and Davis state "introducing any essentially endothermic or dissipative effect opens up the possibility of an eigenvalue solution" [46]. This has been observed for pathological detonations, where the energy release coefficient is negative in portions of the state space, such as for an endothermic reaction or decrease in the number of moles of reaction. However, neither of these situations are expected to exist in detonation of e-PS, and this would be a previously unobserved condition. The eigenvalue, or weak solution, would result in an increase in detonation velocity and a decrease in pressure. While not strictly observed, this cannot be discounted as the pressure in e-PS reactions has not been measured and any changes in detonation velocity would be small and were not detected. The classic CJ detonation structure accounts for the observed detonation velocities within the limits of the experiments when PS pore size is near 3 nm.

Based on experimental agreement seen with CHEETAH-calculated CJ detonation velocities when e-PS pore size is nearest to 3 nm, three main regimes are proposed to exist in fast-reacting e-PS considered here based on initial PS porosity:

1) High porosity, ca. > 70 %. The CJ detonation velocity predicted exceeds the estimated speed of sound in unreacted e-PS. A detonation mechanism consistent with classical CJ theory is plausible and predicted. Experimental observations of propagation rates close to the predicted detonation velocity have been made in a few cases shown in Figure 10. Experiments are limited by difficulty handling PS in this porosity range and synthesizing it with optimal pore size near 3 nm.

2) Low porosity, ca. < 55 %. Speed of sound in unreacted e-PS is estimated to exceed proposed CJ detonation velocities by a factor of > 1.5 and PS strength estimates are similar to or exceeding predicted detonation pressures. Any developed shock would likely decay as sonic waves propagate forward of the shock front into unreacted material. The assumption of insignificant diffusion timescales of reactants owing to extremely small mixing length scale is also weakest in this regime limiting accuracy of the CHEETAH model. Experimental observations in this porosity range with high propagation rates have not been made. While a detonation-like structure similar to regime 3 cannot be fully ruled out, it is most unlikely in this low porosity regime. Deflagration controlled by conduction, convection, and/or crack propagation consistent with conclusions of Parimi et al. [42] is proposed instead.

3) Medium porosity, ca. 55–70 %. Speed of sound in unreacted e-PS and detonation velocities predicted are similar in this transition zone. Flame jumps are most commonly reported experimentally especially at the lower porosity end where sound speed is higher. It is most plausible in this regime that a detonation-like structure unique to e-PS could exist. As discussed in section 3.2, catastrophic failure of the porous structure by a precompression wave, enhanced densification, and shock-induced reaction could support a steady shockwave coupled to the reactive wave that is unable to propagate forward into unreacted material and decay. While this departs significantly from classical detonations wherein the shock is prevented from decaying by the lower relative sound speed ahead, the effect would be similar: a functional pressure spike at the shockwave and rapid chemistry supporting it against natural damping and decay. More investigation is most warranted in this regime to elucidate whether this structure can be observed and whether unique controlling mechanisms exist.

Particularly in the high and medium porosity regimes (regimes 1 and 3 above), plausibility of detonation is supported by a confluence of factors. High reaction rates are evident based on fast propagation rates observed exceed-

ing 1 km/s. Parimi identified the lower activation energy at low heating rates of the fast-propagating variety of e-PS [13]. Elastic compression in solid-solid reaction systems can also significantly lower activation energies as seen in self-propagating high-temperature synthesis reactions [44, 47–49]. The brittle nature of PS and ultimate strength estimates similar to detonation pressures show that rapid catastrophic disintegration of the porous structure could also play a role supporting detonation-like behavior even when sound speed in the unreacted material slightly exceeds the detonation or reactive wave speed. Flame jumps observed are proposed to be a manifestation of this transition zone in the medium porosity range (regime 2).

4 Conclusion

The detonation velocity for energetic porous silicon (PS) with sodium perchlorate oxidizer was estimated according to Chapman-Jouguet (CJ) theory by CHEETAH v9.0 thermochemical software, which computed 1.99 km/s for 69 % silicon porosity. Between 45 % and 85 % PS porosity, this detonation velocity estimate increases from 1.69 km/s to 2.45 km/s. Notably, PS explosive reaction is uniquely low-gas producing. The reaction products predicted at the CJ point are predominantly in the condensed phase, from 86 % by mass at 45 % PS porosity to 46 % by mass at 85 % porosity. The TNT-equivalent mechanical energy is 0.15 to 0.79 on a mass basis limited by low gas release, but total detonation energy in TNT equivalence is 0.73 to 2.0 by mass (2.6 to 5.4 kJ/g thermal energy).

Estimates for the speed of sound in unreacted PS exceed the predicted detonation velocity below 67 % porosity. Above this point, detonation consistent with CJ theory is predicted to be possible and experimental reaction speeds in literature compare to the predicted detonation speed as an upper bound (particularly when pore size is nearest an apparently optimal 3 nm size). At lower porosities a precompression wave is suggested to propagate ahead of a detonation or reaction front. Velocities of discontinuous flame jump ignitions seen ahead of reaction fronts are close to the speed of sound in unreacted PS in this porosity regime, which is the speed at which the precompression wave is expected to propagate. It is possible in the upper region of this porosity range that the detonation wave is strong enough to cause rapid mechanical failure in the PS layer and thus prevent efficient energy transfer to the precompression wave, which may otherwise decay the detonation front.

Therefore, detonation is shown to be feasible in e-PS at porosities above ca. 67 % consistent with CJ theory and at lower porosities with a preceding precompression wave until such forward energy transfer precludes a stable detonation front. Published experimental results agree well with these predictions, which represent an upper-bound of performance possible in optimized e-PS structures. Detonation

pressures predicted between 0.737 and 1.36 GPa varying with porosity are significantly lower than that of conventional military explosives ($>$ 25 GPa), but exceed the highest estimated compression wave amplitude in nanothermites (20 MPa [26, 28]) by two orders of magnitude. Further experimental investigation of reaction pressures would be valuable to test these hypotheses. Nanothermites thus far only exhibit high reaction rates at low densities of 3–20% TMD and quickly slow with densification. e-PS, however, maintains high reaction velocities exceeding 1.5 km/s, theoretically up to over 60% TMD (1.4 g/cm^3), and only weakly slows with densification. The detonation performance estimated for e-PS is even directly comparable to conventional primary explosives at densities below 1 g/cm^3. Porous silicon energetics therefore are proposed to be capable of explosive detonation and represent the most promising metal- or metalloid-based composite energetic for replacement or augmentation of conventional explosives for ignition and initiation systems.

Symbols and Abbreviations

CJ   Chapman-Jouguet
e-PS   Energetic Porous Silicon (PS$+$Oxidizer)
HEL   Hugoniot Elastic Limit
κ Fitting Parameter [19]
LA   Longitudinal Acoustic
ϕ Porosity (Void Fraction)
PS   Porous Silicon
σ Ultimate Strength
SSA   Specific Surface Area
TMD   Theoretical Maximum Density
v Velocity
v_{0LA} LA Velocity in Bulk Silicon [19]

Acknowledgements

Data Availability Statement

Research data are not shared.

References

[1] D. Kovalev, V. Y. Timoshenko, N. Kunzner, E. Gross, F. Koch, Strong explosive interaction of hydrogenated porous silicon with oxygen at cryogenic temperatures, *Physical Review Letters* **2001**, *87*, 068301.

[2] M. J. Sailor, F. V. Mikulec, J. D. Kirtland, *Porous silicon-based explosive*, US Patent 7,942,989, The Regents of the University of California, Oakland, CA, USA **2011**.

[3] N. W. Piekiel, C. J. Morris, W. A. Churaman, D. M. Lunking, B. Fuchs, J. Smyth, E. Cordaro-Gioia, D. Stec, Tailoring porous silicon combustion for lead-free initiators, *Proceedings of the 15th International Detonation Symposium*, July 13–18, **2014**, San Francisco, CA, USA.

[4] L. J. Currano, W. A. Churaman, Energetic nanoporous silicon devices, *Journal of Microelectromechanical Systems* **2009**, *18*, 4, 799–807.

[5] N. W. Piekiel, C. J. Morris, W. A. Churaman, M. E. Cunningham, D. M. Lunking, L. J. Currano, Combustion and material characterization of highly tunable on-chip energetic porous silicon, *Propellants, Explosives, Pyrotechnics* **2015**, *40*, 1, 16–26.

[6] N. W. Piekiel, C. J. Morris, L. J. Currano, D. M. Lunking, B. Isaacson, W. A. Churaman, Enhancement of on-chip combustion via nanoporous silicon microchannels, *Combustion and Flame* **2014**, *161*, 5, 1417–1424.

[7] M. du Plessis, Energetics with Porous Silicon, in: *Handbook of Porous Silicon*, *2nd Edition* (Ed.: L. Canham), Springer International Publishing AG, **2018**, p. 1543–1554.

[8] D. Clement, J. Diener, E. Gross, N. Kunzner, V. Y. Timoshenko, D. Kovalev, Highly explosive nanosilicon-based composite materials, *Physica Status Solidi A* **2005**, *202*, 8, 1357–1364.

[9] A. Abraham, N. W. Piekiel, C. J. Morris, E. L. Dreizin, Combustion of Energetic Porous Silicon Composites Containing Different Oxidizers, *Propellants, Explosives, Pyrotechnics* **2016**, *41*, 1, 179–188.

[10] S. K. Lazaruk, A. V. Dolbik, V. A. Labunov, V. E. Borisenko, Combustion and explosion of nanostructured silicon in microsystem devices, *Semiconductors* **2007**, *41*, 9, 1113–1116.

[11] R. Thiruvengadathan, G. M. Belarde, A. Bezmelnitsyn, M. Shub, W. Balas-Hummers, K. Gangopadhyay, S. Gangopadhyay, Combustion Characteristics of Silicon-Based Nanoenergetic Formulations with Reduced Electrostatic Discharge Sensitivity, *Propellants, Explosives, Pyrotechnics* **2012**, *37*, 3, 359–372.

[12] C. R. Becker, L. J. Currano, W. A. Churaman, C. R. Stoldt, Thermal Analysis of the Exothermic Reaction between Galvanic Porous Silicon and Sodium Perchlorate, *ACS Applied Materials & Interfaces* **2010**, *2*, 11, 2998–3003.

[13] V. S. Parimi, S. A. Tadigadapa, R. A. Yetter, Reactive Wave Propagation Mechanisms in Energetic Porous Silicon Composites, *Combustion Science and Technology* **2015**, *187*, 1–2, 249–268.

[14] I. Glassman, R. A. Yetter, *Combustion*, Elsevier, Burlington, MA, USA **2008**.

[15] P. W. Cooper, *Explosives Engineering*, Wiley-VCH, Weinheim, Germany, **1997**.

[16] R. Friedman, Kinetics of the Combustion Wave, *Journal of American Rocket Society* **1953**, *23*, 6, 349–354.

[17] J. M. D. Lane, A. P. Thompson, T. J. Vogler, Enhanced densification under shock compression in porous silicon, *Physical Review B* **2014**, *90*, 13, 134311.

[18] J. M. D. Lane, A. P. Thompson, T. J. Vogler, Enhanced densification, strength and molecular mechanisms in shock compressed porous silicon, *AIP Conference Proceedings*, Jan 13, **2017**, Tampa Bay, Florida, USA, 120010.

[19] G. N. Aliev, B. Goller, P. A. Snow, Elastic properties of porous silicon studied by acoustic transmission spectroscopy, *Journal of Applied Physics* **2011**, *110*, 4, 043534.

[20] R. J. M. Da Fonseca, J. M. Saurel, A. Foucaran, J. Camassel, E. Massone, T. Taliercio, Y. Boumaiza, Acoustic investigation of porous silicon layers, *Journal of Materials Science* **1995**, *30*, 1, 35–39.

[21] H. J. Fan, M. H. Kuok, S. C. Ng, R. Boukherroub, J.-M. Baribeau, J. W. Fraser, D. J. Lockwood, Brillouin spectroscopy of acoustic modes in porous silicon films, *Physical Review B* **2002**, *65*, 16, 165330.

[22] B. Khasainov, M. Comet, B. Veyssiere, D. Spitzer, Comparison of Performance of Fast-Reacting Nanothermites and Primary Explosives, *Propellants, Explosives, Pyrotechnics* **2017**, *42*, 7, 754–772.

[23] K. S. Martirosyan, L. Wang, A. Vicent, D. Luss, Synthesis and performance of bismuth trioxide nanoparticles for high energy gas generator use, *Nanotechnology* **2009**, *20*, 40, 405609.

[24] K. S. Martirosyan, Nanoenergetic Gas-Generators: principles and applications, *Journal of Materials Chemistry* **2011**, *21*, 26, 9400.

[25] R. Shende, S. Subramanian, S. Hasan, S. Apperson, R. Thiruvengadathan, K. Gangopadhyay, S. Gangopadhyay, P. Redner, D. Kapoor, S. Nicolich, W. Balas, Nanoenergetic Composites of CuO Nanorods, Nanowires, and Al-Nanoparticles, *Propellants, Explosives, Pyrotechnics* **2008**, *33*, 2, 122–130.

[26] S. Apperson, R. V. Shende, S. Subramanian, D. Tappmeyer, S. Gangopadhyay, Z. Chen, K. Gangopadhyay, P. Redner, S. Nicholich, D. Kapoor, Generation of fast propagating combustion and shock waves with copper oxide/aluminum nanothermite composites, *Applied Physics Letters* **2007**, *91*, 24, 243109.

[27] K. T. Sullivan, N. W. Piekiel, S. Chowdhury, C. Wu, M. R. Zachariah, C. E. Johnson, Ignition and Combustion Characteristics of Nanoscale Al/AgIO3 : A Potential Energetic Biocidal System, *Combustion Science and Technology* **2010**, *183*, 3, 285–302.

[28] B. S. Bockmon, M. L. Pantoya, S. F. Son, B. W. Asay, J. T. Mang, Combustion velocities and propagation mechanisms of metastable interstitial composites, *Journal of Applied Physics* **2005**, *98*, 6, 064903.

[29] D. Prentice, M. L. Pantoya, A. E. Gash, Combustion Wave Speeds of Sol Gel-Synthesized Tungsten Trioxide and Nano-Aluminum: The Effect of Impurities on Flame Propagation, *Energy & Fuels* **2006**, *20*, 6, 2370–2376.

[30] S. Bastea, L. E. Fried, K. R. Glaesemann, W. M. Howard, I.-F. W. Kuo, S. Nimmakayala, P. C. Souers, D. Taller, P. A. Vitello, *CHEETAH 9.0 Thermochemical Code*, **2019**, Energetic Materials Center, Lawrence Livermore National Laboratory, Livermore, CA, USA.

[31] D. Feller, D. A. Dixon, Theoretical Study of the Heats of Formation of Small Silicon-Containing Compounds, *Journal of Physical Chemistry A* **1999**, *103*, 32, 6413–6419.

[32] L. Canham, Microporous Silicon, in: *Handbook of Porous Silicon, 2nd Edition* (Ed.: L. Canham), Springer International Publishing AG **2018**, p. 149–155.

[33] W. H. Gust, E. B. Royce, Axial Yield Strengths and Two Successive Phase Transition Stresses for Crystalline Silicon, *Journal of Applied Physics* **1971**, *42*, 5, 1897–1905.

[34] S. J. Turneaure, S. M. Sharma, Y. Gupta, Nanosecond Melting and Recrystallization in Shock-Compressed Silicon, *Physical Review Letters* **2018**, *121*, 13, 135701.

[35] R. F. Smith, R. W. Minich, R. E. Rudd, J. H. Eggert, C. A. Bolme, S. L. Brygoo, A. M. Jones, G. W. Collins, Orientation and rate de-

[36] L. Canham, Mechanical Properties of Porous Silicon, in: *Handbook of Porous Silicon, 2nd Edition* (Ed.: L. Canham), Springer International Publishing AG **2018**, p. 309–318.

[37] A. Klyshko, M. Balucani, A. Ferrari, Mechanical strength of porous silicon and its possible applications, *Superlattices and Microstructures* **2008**, *44*, 4–5, 374–377.

[38] D. C. Miller, B. L. Boyce, P. G. Kotula, C. R. Stoldt, Connections between morphological and mechanical evolution during galvanic corrosion of micromachined polycrystalline and monocrystalline silicon, *Journal of Applied Physics* **2008**, *103*, 12, 123518.

[39] F. Wang, K. Zhao, J. Cheng, J. Zhang, Conciliating surface superhydrophobicities and mechanical strength of porous silicon films, *Applied Surface Science* **2011**, *257*, 7, 2752–2755.

[40] A. Plummer, V. Kuznetsov, T. Joyner, J. Shapter, N. H. Voelcker, The Burning Rate of Energetic Films of Nanostructured Porous Silicon, *Small* **2011**, *7*, 23, 3392–3398.

[41] R. Van Riet, E. Amayuelas, P. Lodewyckx, M. H. Lefebvre, C. O. Ania, Novel opportunities for nanoporous carbons as energetic materials, *Carbon* **2020**, *164*, 129–132.

[42] V. Parimi, Characterization of Porous Silicon for Micropyrotechnic Applications, Doctoral Dissertation, Penn State University, *Electronic Theses and Dissertations for Graduate School* **2015**.

[43] J. M. Densmore, K. T. Sullivan, A. E. Gash, J. D. Kuntz. Expansion behavior and temperature mapping of thermites in burn tubes as a function of fill length, *Propellants, Explosives, Pyrotechnics* **2014**, *39*, 3, 416–422.

[44] H. J. Viljoen, V. Hlavacek. Deflagration and detonation in solid-solid combustion, *AIChE journal* **1997**, *43*, 11, 3085–94.

[45] J. J. Davis, A. J. Lindfors, P. J. Miller, S. Finnegan, D. L. Woody. Detonation like phenomena in metal-polymer and metal/metal oxide-polymer mixtures, *Proceedings of the 11th International Detonation Symposium*, August 30 – September 4, **1998**, Snowmass, CO, USA.

[46] W. Fickett, W. C. Davis. *Detonation: Theory and Experiment*, Dover Publications, Inc., **1979**.

[47] J. R. Bielenberg, H. J. Viljoen. Chemo-mechanical interaction in solid-solid reactions, *AIChE journal* **1999**, *45*, 5, 1072–84.

[48] V. A. Benderskii, P. G. Filippov, M. A. Ovchinnikov, Ratio of Thermal and Deformation Ignition in Low-Temperature Solid-Phase Reactions, *Doklady Akud. Nauk SSSR* **1989**, *308*, 2, 401.

[49] N. S. Enikolopyan, A. I. Aleksandrov, E. E. Gasparyan, V. I. Shelobkov, A. A, Direct Conversion of Chemical Energy into Mechanical without Thermalization, *Doklady Akad. Nauk SSSR* **1991**, *319*, 6, 1384.